**Showcasing research from Dr. Saito's team, at the Chemical Sciences Division in Oak Ridge National Laboratory, Oak Ridge, Tennessee, USA.**

Understanding and tuning organocatalysts for versatile condensation polymer deconstruction

The application of linear free energy relationships, i.e. Hammett analysis, reveals a design principle of organocatalysts for condensation polymer deconstruction. The findings identify triazabicyclodecene:para-aminobenzoic acid (TBD:PABA) as the most effective catalyst, where PABA is an economical and abundant compound known as vitamin B-10. TBD:PABA enables selective deconstruction of polycarbonate, PET, and Nylon as well as variety of mixed plastics, providing a scalable and sustainable solution for managing variety of plastic wastes.

Image reproduced by permission of Adam Malin and Oak Ridge National Laboratory from *J. Mater. Chem. A,* 2025, **13**, 32111.

As featured in:
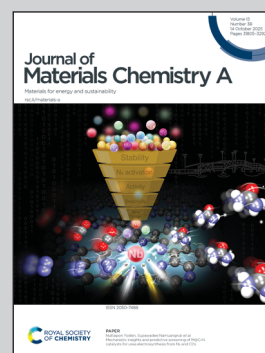
See Tomonori Saito *et al.,*
J. Mater. Chem. A, 2025, **13**, 32111.

ROYAL SOCIETY
OF **CHEMISTRY**

rsc.li/materials-a

COMMUNICATION

Check for updates

Understanding and tuning organocatalysts for versatile condensation polymer deconstruction†

Jackie Zheng,‡[ab] Octavio Jupp,‡[b] Nicholas J. Galan,‡[b] Bobby G. Sumpter, [ID][c] Sheng Dai, [ID][b] Jeffrey C. Foster [ID][b] and Tomonori Saito [ID]*[ab]

Plastics are widely used for their durability and versatility, but recycling remains a major challenge, especially for mixed or contaminated waste. Mechanical recycling works well for clean, single-polymer streams like PET but has limited efficiency for complex waste streams. Chemical recycling, particularly glycolysis, is often employed to selectively deconstruct condensation polymers under mild conditions. This study explores catalyst design for glycolysis using linear free energy (Hammett) analysis to evaluate how catalyst structure influences polymer deconstruction. Polycaprolactone (PCL) is used as a model polyester due to its solubility and low deconstruction temperature. Triazabicyclodecene (TBD) paired with benzoic acid derivatives depicts a clear linear trend in depolymerization rates with Hammett values. TBD with *p*-aminobenzoic acid (PABA) stands out for its catalytic efficiency, thermal stability, and scalability, along with PABA's commercial availability as vitamin B-10. The TBD : PABA catalyst not only effectively breaks down PCL but also enables sequential deconstruction of polycarbonate, PET, and Nylon in mixed waste streams. These results highlight the value of Hammett-guided catalyst design and establish TBD : PABA as a promising, scalable organocatalyst for mixed plastic recycling, enabling recovery of individual polymer building blocks from blended waste and offering a practical route toward circular plastics.

[a]Bredesen Center for Interdisciplinary Research and Education, University of Tennessee, Knoxville, Knoxville, TN 37966, USA

[b]Chemical Sciences Division, Oak Ridge National Laboratory, Oak Ridge, TN 37831, USA

[c]Center for Nanophase Materials Sciences, Oak Ridge National Laboratory, Oak Ridge, TN 37831, USA

‡ Equal contribution.

Introduction

Plastic materials are integral to modern society. They are widely utilized across various industries due to their lightweight, durable, scalable and versatile nature. From packaging and automotive parts to electronics and medical devices, plastics offer a broad range of functional advantages that make them indispensable. As such, over 413 million metric tons of plastic were produced in 2023.[1] However, these same characteristics, durability and resistance to degradation, present significant challenges when it comes to managing plastic waste, particularly at their end of life. Only ~9% of global plastics are recycled, with most of the plastic waste either incinerated, landfilled or discarded into the environment.[2] The accumulation of plastic waste in landfills and the environment, coupled with the limited capacity of traditional recycling methods, has become a pressing global challenge.[3]

Current recycling efforts are often hindered by the complexity and heterogeneity of plastic waste. The variety of polymer types, each with unique chemical structures, requires distinct processing methods and temperatures, complicating the recycling process.[4] Mechanical recycling, the most common approach, involves shredding, melting, and reusing plastic materials. However, this method is often limited by contamination, thermal and mechanical degradation during processing, and the inability to recycle multi-polymer blends or mixed plastics effectively, where many plastics exist as such mixed state (Fig. 1).[4,5]

To address these challenges, chemical recycling has emerged as a promising solution.[6–9] Unlike mechanical methods, chemical recycling deconstructs polymers into their monomeric or oligomeric constituents, enabling the reintegration of end-of-life materials back into manufacturing processes. This approach offers greater flexibility in processing a wide variety of plastics,[7] including those that are difficult to recycle mechanically. Among the chemical recycling techniques, glycolysis is an effective path to efficiently depolymerize certain plastics, such as polyesters and polycarbonates, using specific catalysts (Fig. 1).[7,10]

This journal is © The Royal Society of Chemistry 2025

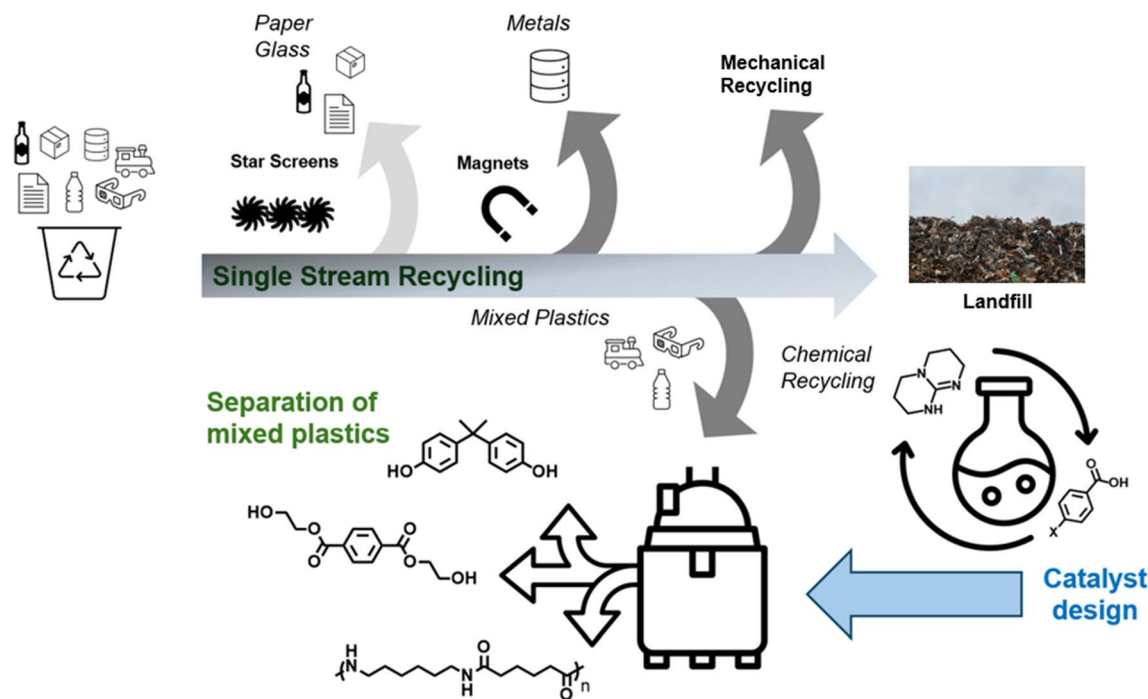*J. Mater. Chem. A*, 2025, 13, 32111–32121 | 32111

Fig. 1 Chemical recycling can be used to process mixed plastics after metals, papers, and glass have been sorted out from single stream recycling feedstocks. Selective glycolysis can process mixed plastic streams. Landfill photograph by Emmet from Pexels.com. Energy and catalyst icons: Flaticon.com.

A significant limitation in advancing chemical recycling lies in the design and optimization of deconstruction catalysts. Catalysts such as 1,5,7-triazabicyclo[4.4.0]dec-5-ene (TBD)[11] have demonstrated high efficiency in facilitating glycolysis but suffer from thermal degradation and hydrolytic instability,[12] which limits their reusability and commercial applicability. Previous studies have shown that combining TBD, or similar organobases, with acids to form protic organic salts can enhance their thermal stability, reusability, and their catalytic performance at high temperature.[7,8,13] Among these, TBD : trifluoroacetic acid (TBD : TFA)[7] and TBD : methanesulfonic acid (TBD : MSA)[6] have emerged as effective systems. The high efficiency of TBD : TFA and TBD : MSA catalysts allow for the deconstruction of multiple condensation polymers such as poly(ethylene terephthalate) (PET), polyamide (PA), polyurethane (PU), and polycarbonate (PC), however, the underlying mechanisms and performance differences driven by the chemical structure of the acid counterion in protic organo salt catalysts remain poorly understood.

To address the knowledge gap in catalyst design for plastic glycolysis, this study employs Hammett analysis[14] to investigate how substituent effects and pK_a differences of acid counterions influence the performance of TBD : acid organocatalysts (Fig. 1), which has never been applied to polymer deconstruction to the best of our knowledge. While some trend for the basicity (*i.e.* pK_a) of common organobases such as TBD, 1,8-diazabicyclo[5.4.0]undec-7-ene (DBU), and 4-dimethylaminopyridine (DMAP) *etc.* have been reported,[15] the design principle for selecting the acid pair for organobase salts for polymer deconstruction has not been well understood with little

investigation.[16] To systematically investigate the role of acid counterions in protic organo salt catalysts, benzoic acid derivatives were selected as model acids due to their well-tabulated substituent parameters and broad range of pK_a values, providing a systematic framework to assess the impact of electron-donating and electron-withdrawing groups on catalytic activity and thermal stability. The Hammett plot (or linear free energy relationship), a well-established tool for evaluating electronic influences on reaction rates and equilibrium constants, enables a quantitative correlation between substituent effects and catalyst performance.[17] By integrating kinetic data with these electronic trends, this study aims to expand the toolbox of guiding principles for designing thermally stable, efficient, and cost-effective catalysts for chemical recycling (Fig. 1). Furthermore, benzoic acid derivatives offer practical advantages over other acids previously reported, including availability, lower cost, and reduced toxicity, making them attractive candidates for scalable and sustainable catalyst development for polymer deconstruction.

In the first part of this study, poly(caprolactone) (PCL), was systematically deconstructed using various combinations of TBD and benzoic acid derivatives to understand substituent effects on depolymerization kinetics. PCL was selected as the model polymer due to its solubility in many organic solvents, enabling accurate kinetic monitoring on homogeneous deconstruction reactions.[18] 4-Aminobenzoic acid (PABA), 4-methoxybenzoic acid (MeOBA), *p*-toluic acid (TA), benzoic acid (BA), and 4-(trifluoromethyl)-benzoic acid (TFMBA) were selected as the acids to study (Scheme 1), where the functional groups at the *para*-position of these benzoic acid derivatives covered a range
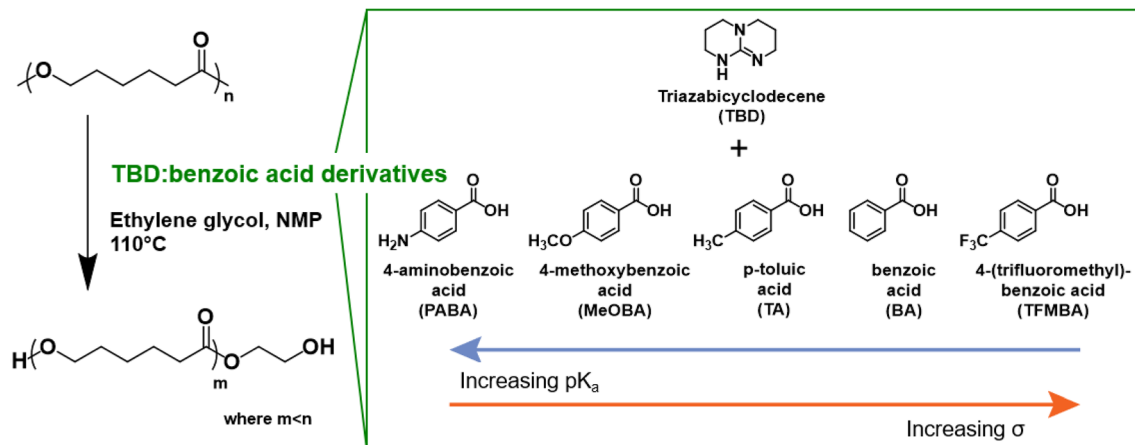
Scheme 1 Chemical deconstruction of PCL using TBD : benzoic acid derivatives.

of pK_a values from 3.7–5.0 and a range of Hammett substituent constants from −0.66 to 0.54. Rate constants obtained from fitting deconstruction kinetics were compared to the rate of TBD : BA and the logarithm of these results were plotted against the corresponding substituent constant, σ, to determine the proportionality constant, ρ. The results of the Hammett analysis enable a predictive approach to catalyst design, which is further reinforced through thermal analysis, revealing that the protic organic salts prepared herein exhibit enhanced stability compared to TBD alone. Following catalyst optimization, we further demonstrated sequential deconstruction for other commercially relevant condensation polymers such as PET, PC, and Nylon. Additionally, the process can selectively deconstruct mixed plastics waste, including selective deconstruction of PET with full recovery of inert plastics such as polyolefins from the mixture of polyester fabric, plastic tab, and plastic bag, and selective deconstruction of PET and nylon fibers from post-consumer mixed plastics waste such as automobile floor mat fibers and mixed fabric clothing.

The insights from this study have important implications for the chemical recycling of plastics. Understanding the design principles of organocatalysts through Hammett analysis is crucial for developing a strategic approach to creating novel catalysts that can efficiently deconstruct mixed plastics in a single reactor, while also enabling effective separation—

tackling key challenges in plastic waste sorting and processing.[4,7,19,20] Such advancements would enable the broader deployment of chemical recycling technologies, contributing to a circular economy for plastics.

Results and discussion

Impact of anion electronic structure in TBD-based organocatalysts during PCL deconstruction

The selected benzoic acid substituents (Scheme 1) exhibit diverse electron-donating and withdrawing properties, influencing their pK_a values, which range from 3.7 to 5.0, compared to unsubstituted benzoic acid at 4.2 (Table 1). These electronic effects are quantified by Hammett σ values—PABA (−0.66), MeOBA (−0.27), TA (−0.17), BA (0), and TFMBA (0.54) (Table 1)—which reflect the ability of substituents to stabilize or destabilize charge through resonance and inductive effects. Hammett analysis is a powerful tool for understanding reaction mechanisms and reaction sensitivity to electronic effects, yet it is rarely applied in catalysis for polymer deconstruction. By correlating electronic properties with catalytic activity and stability, this approach provides predictive insight, enabling the rational design of catalysts that meet specific performance constraints such as thermal stability at elevated deconstruction temperatures.

Table 1 Property of acids and their TBD : acid complex

Acid	$pK_a{}^a$	σ-Value[b]	$k_x{}^c$	$\log(k_x/k_H)$	$T_{d,5\%}$ (°C)	T_m (°C)	Binding energy[d] (kcal mol^{-1})
PABA	5.0	−0.66	−2.85	0.54	251	104	17.05 (11.9)[e]
MeOBa	4.5	−0.27	−1.54	0.27	184	116	19.03
TA	4.3	−0.17	−1.25	0.18	187	133	19.39
BA	4.2	0	−0.82	0	184	130	18.92
TFMBA	3.7	0.54	−0.22	−0.57	210	156	21.22

[a] pK_a value in water as found on vendor websites. [b] Tabulated by Hammett.[14] [c] Calculated *via* the slope of the linear fit of the logarithm of kinetics data. [d] Binding energies were calculated by DFT. [e] The value listed in parenthesis for the binding energy of the alternate coordination of PABA with TBD, where the amino-group is coordinated with TBD.

This journal is © The Royal Society of Chemistry 2025

J. Mater. Chem. A, 2025, 13, 32111–32121 | 32113

The thermal stability of organosalts typically reflects their dissociation equilibria and suggests their usable temperature range. Increased thermal stability enables deconstruction reactions at higher temperatures avoiding catalyst thermal decomposition and potentially allows for higher temperatures and shorter reaction times for chemical recycling. The thermal stability of the TBD : benzoic acid derivatives were measured *via* thermogravimetric analysis (TGA) at a heating rate of 5 °C min^{-1} (Fig. 2A). The organosalt decomposition temperature (T_d) can be tuned by the type of benzoic acid derivative pairing with TBD, which exhibits middling thermal stability in comparison ($T_{d,5\%}$ = 103 °C). TBD : BA, TBD : MeOBA, TBD : TA showed similar $T_{d,5\%}$ near 185 °C, while TBD : TFMBA and TBD : PABA exhibited $T_{d,5\%}$ = 210 °C and 251 °C, respectively. All of these TBD : benzoic acid derivatives (TBD : BA, TBD : MeOBA, TBD : TA, TBD : TFMBA, TBD : PABA) exhibit higher thermal stability than our previously reported TBD : TFA ($T_{d,5\%}$ = 177 °C).[7] High thermal stability of TBD : PABA, the most stable TBD : benzoic acid derivative in this study, was further supported by an isothermal experiment, where TBD : TFA and TBD : PABA were heated to 180 °C (5 °C min^{-1}) and held at 180 °C for 180 min. More than 95% of TBD : TFA was decomposed within 54 min (after isotherm), whereas TBD : PABA exhibited a ~2 wt% change after 180 min (Fig. 2B). Taken together, these data suggest that TBD : PABA exhibits significantly improved thermal stability compared to standalone TBD or TBD : TFA, which is desirable for deconstruction catalysts.

Density functional theory (DFT) calculations were performed for each acid–base pair in the gas phase to determine their binding energies, which correlated with the pK_a difference between TBD (pK_a ~ 26) and the corresponding benzoic acid derivative (Table 1). A larger pK_a difference resulted in higher
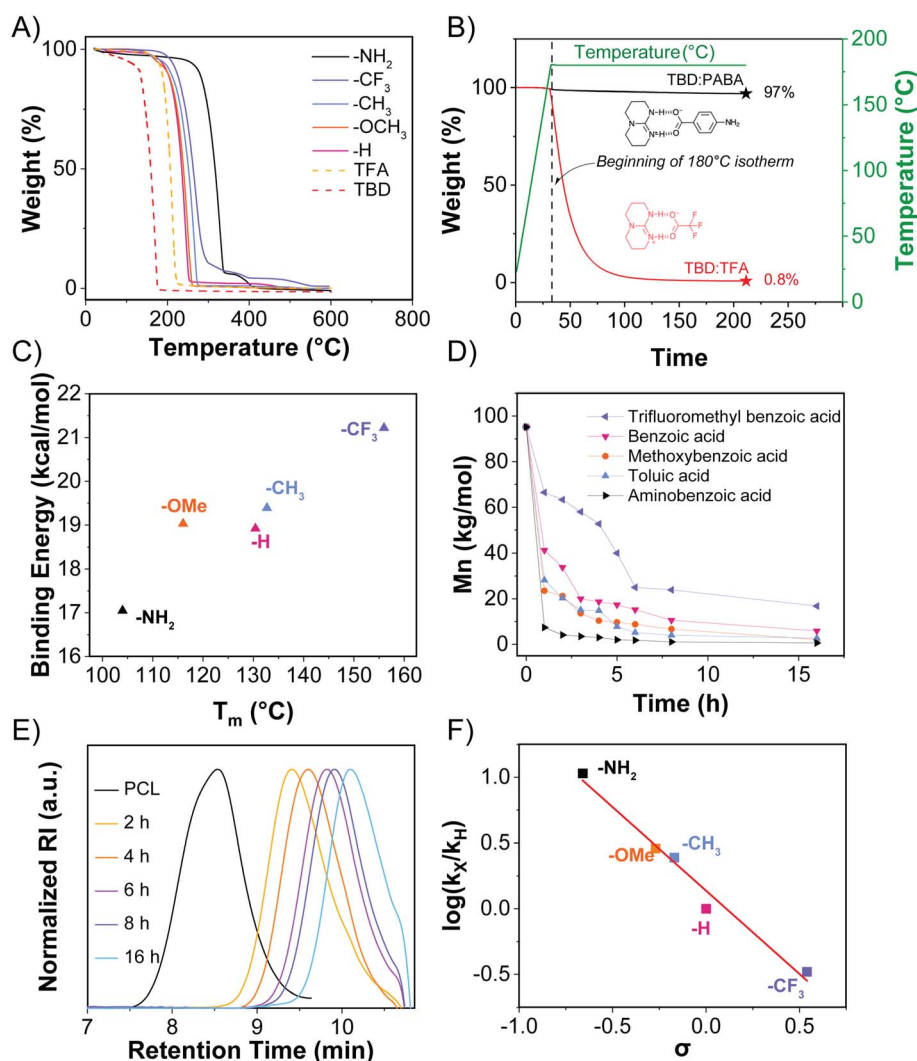

Fig. 2 (A) TGA thermograms depicting the thermal stability of the various TBD : benzoic acid catalysts used in this study. (B) Isothermal TGA thermogram highlighting the enhanced thermal stability of TBD : PABA. (C) DFT calculations show a correlation between binding energy and T_m. (D) Deconstruction kinetics of each acid are measured by tracking changes M_n in *via* SEC measurements. (E) Selected SEC traces for TBD : PABA mediated glycolysis of PCL. (F) Hammett plot based on apparent rate constants calculated from kinetics experiment in figure (D).

32114 | *J. Mater. Chem. A*, 2025, **13**, 32111–32121

This journal is © The Royal Society of Chemistry 2025

binding energy (Table 1), consistent with previously reported trends for ionic liquids.[21,22] Moreover, it should be noted that the binding energies increase as the substituents become more electronegative, further supporting that stronger acids lead to stronger interactions with TBD. These calculations also revealed a positive correlation between binding energy and catalyst thermal stability (T_d), except for PABA (Fig. S1). While TBD : PABA showed the highest T_d, it also had the lowest binding energy of 17.05 kcal mol^{-1}. To better understand this difference, differential scanning calorimetry (DSC) was conducted to determine melting temperatures of each TBD : acid organocatalyst, and it was found that TBD : MeOBA had a melting point of 116 °C, TBD : TA = 133 °C, TBD : BA = 130 °C, and TBD : TFMBA = 156 °C (Fig. S2–S6), fitting a similar trend of lower pK_a have higher melting points, and roughly corresponding to the trend in binding energy (Fig. 2C).

The melting point of TBD : PABA was determined to be 104 °C, aligning with the observed binding energy vs. melting point trend (Fig. 2C). However, its DSC trace exhibited an unexpected exotherm at 176 °C (Fig. S2). This exotherm may explain why TBD : PABA has the highest T_d among these TBD : acid organocatalysts despite its low binding energy, as alternative binding modalities of the complex could enhance its thermal stability. DFT calculations suggested that PABA could reorient and coordinate with TBD via the amine group as an alternate binding modality (Fig. S7).

To evaluate the impact of acid substitution on catalytic activity for the TBD : acid organocatalysts, kinetic experiments of PCL (M_n = 95.2 kg mol^{-1}, Đ = 1.86) glycolysis were conducted. Kinetic experiments were performed under homogeneous conditions to eliminate variables such as mass-transfer limitations due to polymer particle size. PCL was dissolved in N-methylpyrrolidone (NMP), a suitable high-boiling solvent to enable homogeneous PCL glycolysis, at 110 °C before ethylene glycol was added. After the solution appeared homogeneous again, the TBD and the appropriate acid were added in 1 : 1 stoichiometry. Prior to conducting the kinetic experiments, we compared the deconstruction efficiency of an isolated protic organic salt (TBD : acid organocatalysts, Fig. S8) and one prepared in situ by adding acid and base (TBD) one by one to the reaction solution. No significant differences in apparent reaction rates were observed (Fig. S8), thus, we prepared the TBD organocatalysts in situ for the remainder of this study, unless otherwise noted, for simplicity and consistency (note: some of the TBD : acid catalysts were difficult to fully dry and isolate).

Reaction progress was monitored by tracking changes in polymer molecular weight as a function of time using size exclusion chromatography (SEC, Fig. 2D, E and S9–S13). An apparent time-dependent exponential decrease in molecular weight for the deconstruction reactions suggested that polymer cleavage occurred predominately through a random scission mechanism. Trends in the observed deconstruction kinetic behavior correlated well with acid pK_a, with higher pK_a values corresponding to higher ultimate conversions. Final molecular weights after 16 h further supported this trend, where TBD : TFMBA had the highest final molecular weight (M_n) of 16.8 kg mol^{-1} and TBD : PABA had the lowest final molecular weight of 600 g mol^{-1}. This correlation likely originates from the conjugate basicity of the acids—weaker acids form more stable bases that bind less strongly to TBD, leaving it more available to activate ethylene glycol for deconstruction. In addition to affording the lowest final molecular weight, TBD : PABA also exhibited the most drastic change in molecular weight early in the deconstruction reaction, reducing molecular weight from 95.2 kg mol^{-1} to 7.4 kg mol^{-1} within 1 h. To ensure PABA was not capable of aminolysis by itself, a control experiment with excess amounts of PABA was conducted, but there was no change in PCL molecular weight observed (Fig. S14).

To determine apparent rate constants, the conversion at each time point was calculated based on the starting molecular weight and the logarithm of the conversion was plotted against reaction time (Fig. S15). The slope of each fit was used as the k_x value (Table 1), which were then plotted against the corresponding σ-values (Fig. 2F). The slope of the fitted linear regression was used to determine the proportionality constant, ρ, representing the reaction's sensitivity to electronic effects (Fig. 2F). The resulting ρ = −1.26 indicated that electron-donating substituents enhance the reaction rate by destabilizing the negative charge on the carboxylate, which raises their pK_a and leads to lower binding energies. The protic salts with lower binding energy (Table 1 and Fig. 2C) allow easier dissociation from TBD during the deconstruction process, which is mechanistically important for condensation polymer deconstruction,[7] and their trend correspond well to electronic effects on the deconstruction rate (Fig. 2F).

Mixed plastic deconstruction

Many different types of polymers are present in everyday consumer products. Due to the similarity in appearance and properties of these plastics, post-consumer waste intended for recycling is rarely separated by plastic type. Instead, it often exists as a single-stream waste, where papers, plastics, and metals are mixed, or as a collection where plastics are separated from other recyclables but not categorized by type (Fig. 1).[4,23] To test the capability of our TBD : PABA catalyst to deconstruct mixed plastic types, we started by deconstructing PET using conditions previously reported for TBD : TFA,[7] and we found that TBD : PABA showed similar performance (Fig. S16 and S17). As such, we expanded our experiments to deconstruct other types of polymers including PC and Nylon. Similarly to our previous report,[7] we can deconstruct various types of condensation polymers commonly found in post-consumer plastic waste.

To demonstrate the applicability of TBD : PABA for addressing single-stream mixed plastic waste, a sequential and selective deconstruction experiment was conducted using a mixture of poly(bisphenol A carbonate) (PC, M_w = 40 000 g mol^{-1}), poly(ethylene terephthalate) (PET, M_w = 60 000 g mol^{-1}), and Nylon 6,6 (M_w = 84 700 g mol^{-1}). These polymers were chosen as representative condensation polymers due to their widespread use in consumer goods such as car parts, bottles, clothing, and carpets, where the majority exist as mixed plastics. Deconstruction experiments were first conducted individually, where

This journal is © The Royal Society of Chemistry 2025

J. Mater. Chem. A, 2025, 13, 32111–32121 | 32115

each polymer was added to a pressure tube containing a stock solution of ethylene glycol, the TBD : PABA catalyst, and trimethoxybenzene as an internal standard with no additional solvent. The temperature-dependent deconstruction reactions were carried out at 140 °C for PC, 190 °C for PET, and 230 °C for Nylon 6,6. After individual deconstruction, a mixed plastic deconstruction experiment was performed by combining all three plastics into a single pressure vessel, which was heated stepwise to their respective deconstruction temperatures (Fig. 3). All reactions were conducted at temperatures that allowed complete deconstruction of the target polymer within 2 hours, enabling real-time monitoring via ^{1}H NMR and SEC.

To track the reaction progress of PC deconstruction, aliquots were taken every 30 min and dissolved in CDCl$_3$ to track the formation of bisphenol A (BPA) via ^{1}H NMR spectroscopy. Since PET and Nylon 6,6 remained intact after the PC deconstruction, the residue was suspended in CHCl$_3$ to recover the BPA product and to remove various carbonate byproducts including ethylene carbonate (Fig. S18–S21). Unreacted PET and Nylon 6,6 were isolated from this mixture via simple vacuum filtration. The polymeric solids were returned to the pressure tube with fresh

catalyst solution for subsequent reactions to deconstruct PET (190 °C) and later Nylon 6,6 (230 °C).

While the PET and Nylon 6,6 remained completely intact at 140 °C, Nylon 6,6 melts during the 190 °C deconstruction of PET. Therefore, instead of collecting aliquots for kinetic sampling, the reactions were stopped every 30 min, and the pressure tubes were cooled to halt the deconstruction process. Deuterated dimethylsulfoxide (DMSO-d$_6$) was added to the pressure tubes, and any clumps of Nylon 6,6 were broken up to dissolve entrapped bis(2-hydroxyethyl) terephthalate (BHET) formed during the reaction, the pressure tube was sonicated for 30 minutes to ensure particles were broken apart and BHET dissolved in DMSO-d$_6$. Conversion to BHET was monitored by both the appearance of aromatic peaks as well as methylene peaks (Fig. S22–S25). Following 2 h at 190 °C, most of the PET was converted into BHET, leaving behind only Nylon 6,6 particles. The recovered Nylon powder was further deconstructed at 230 °C to lower molecular weight polymers and oligomers by adding additional ethylene glycol/catalyst solution.

In contrast to PC and PET, Nylon 6,6 exhibited a different behavior during the deconstruction at 190 °C and 230 °C. When immersed in EG, Nylon 6,6 melted at significantly lower
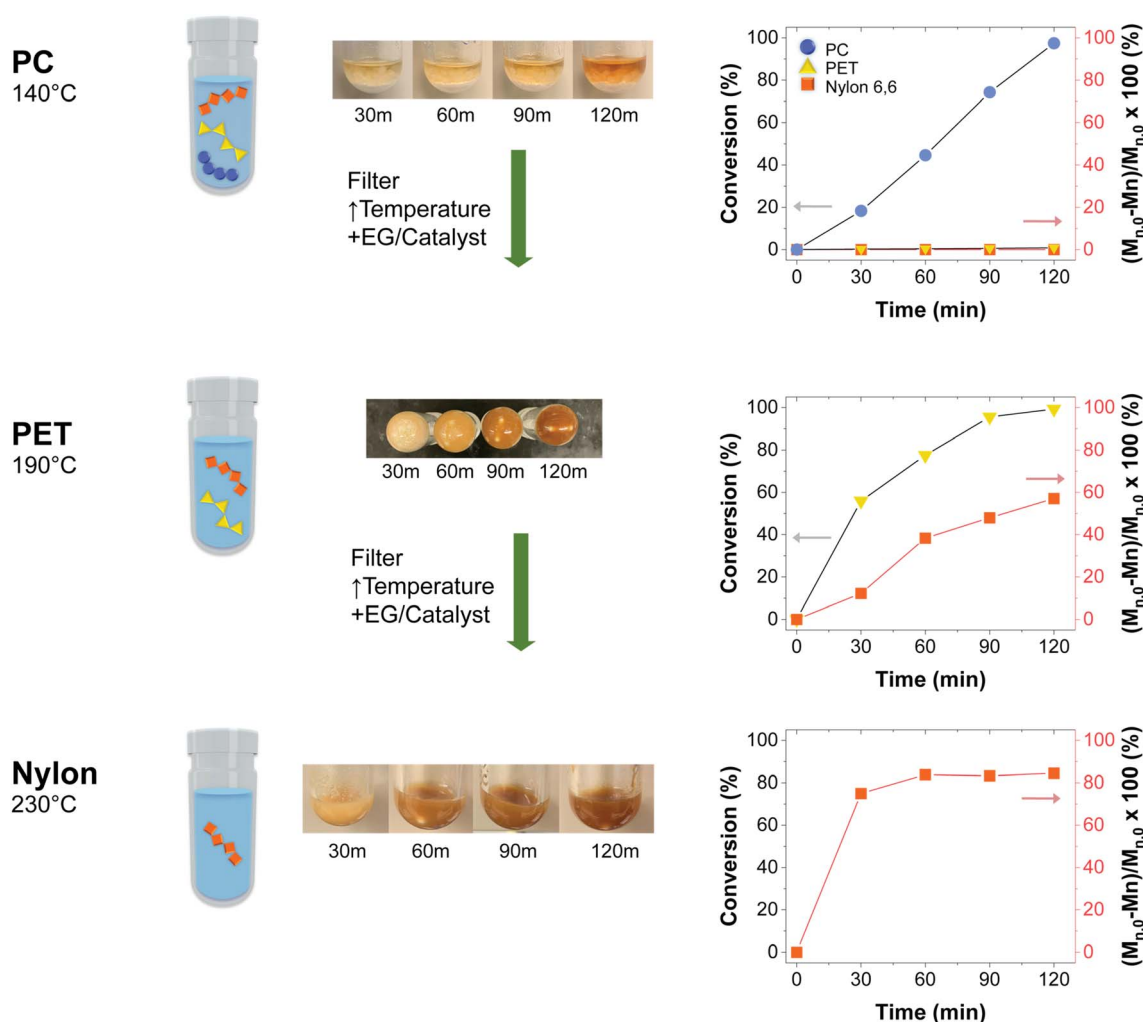

Fig. 3 Changing temperature enables the selective and sequential deconstruction of PC, PET, and Nylon 6,6.

32116 | J. Mater. Chem. A, 2025, 13, 32111–32121

This journal is © The Royal Society of Chemistry 2025

temperatures, and even partially depolymerized at 190 °C, facilitating a more homogeneous deconstruction compared with PC and PET. The deconstruction of Nylon 6,6 appeared to reach an equilibrium molecular weight[24] of $M_n = 2.1$ kg mol^{-1} through random backbone scission, and possible occurrence of reversible polymerization, preventing complete depolymerization into monomers, in contrast to our observations for PC and PET deconstruction. Consequently, instead of reporting conversion, the change in Nylon 6,6 molecular weight was measured by HFIP-SEC by dissolving the recovered Nylon solids in hexafluoroisopropanol (HFIP, Fig. S26 and S27).

The final molecular weight of $M_n = 2.1$ kg mol^{-1} after 2 hours at 230 °C suggests that TBD : PABA is a competent catalyst for Nylon 6,6 glycolysis. The only other report found in literature for glycolysis of Nylon 6,6 by Kim *et al.* reported $M_n \approx 5$ kg mol^{-1} after 8 hours at 275 °C.[24] Despite the difference of EG ratio, 2 : 1 excess in their study *versus* 10 : 1 excess in our study, our study here using TBD : PABA reached equilibrium molecular weight after 1 hour, while previous reports needed 6 hours. Additionally, our deconstruction was conducted at a lower temperature of 230 °C, while prior work required a higher temperature of 275 °C, further highlighting the efficiency of glycolysis by TBD : PABA. To further demonstrate efficacy of our catalyst for the observed Nylon 6,6 deconstruction, we conducted Nylon 6,6 glycolysis with and without TBD : PABA at 230 °C. While Nylon 6,6 deconstruction was observed also for EG alone without catalyst, Nylon 6,6 glycolysis with TBD : PABA exhibited faster deconstruction kinetics (Fig. S28).

Mixed plastic waste streams were also tested by preparing a sample containing a poly(propylene) cap tab, a poly(ethylene) plastic bag, and a piece of PET fabric (Fig. 4A). The mixture was added to a pressure vessel with 3 mL of EG and TBD : PABA and heated at 190 °C. Within 30 minutes, the PET fabric was fully deconstructed, while the polypropylene and polyethylene remained unreacted and were quantitatively recovered by mass. We further demonstrated the versatility of TBD : PABA catalyst by deconstructing mixed post-consumer waste such as fibers from an automobile floor mat, consisting of both polyester and Nylon, and portions of a mixed fabric shirt composed of 50 : 50 cotton and polyester. The floor mat was pretreated by shearing the fibers off the PE backing and subjecting them to the conditions used for Nylon 6,6 deconstruction. After 2 h, the reaction was cooled to RT and the residue was dissolved in HFIP (Fig. 4B) and sampled for SEC analysis, which revealed an 88% reduction in molecular weight of Nylon 6,6 from 32 300 to 3800 g mol^{-1} (Fig. S29), while the fully deconstructed polyester remained in solution. The ~50% polyester, ~50% cotton mixed fabric shirt (2.5 g total weight) was cut into pieces and deconstructed at 190 °C for 2 h (note: 20 equiv. of EG were used for these post-consumer materials to submerge the sample). The reaction mixture was cooled to RT and diluted with tetrahydrofuran (THF), resulting in 1.19 g of the unreacted cotton (Fig. 4C), roughly corresponding to the composition. The polyester portion was fully deconstructed, as no detectable polymer was observed in the subsequent SEC trace (Fig. S30). These data further demonstrate that TBD : PABA can act as a versatile catalyst resistant to the additives present in post-consumer waste plastics.

Facile scalability of TBD : PABA

We further demonstrated facile preparation of TBD : PABA salt by dissolving TBD and PABA individually in THF. Upon mixing, a precipitate formed, indicating the formation of a 1 : 1 molar ratio salt (Movie S1), while excess TBD or PABA remained soluble in THF. The salt was isolated by vacuum filtration, washed with additional THF, and dried under vacuum. ^{1}H NMR spectroscopy confirmed peak integrations consistent with 1 : 1 salt formation (Fig. 4D). Compared to previously reported catalysts such as TBD : TFA, the TBD : PABA catalyst offers the advantage of not requiring thermal management, as no observable excessive heat is produced that could evaporate volatile compounds like TFA. As such, it was possible to readily increase the scale of the salt synthesis to 10 g in open beakers without additional equipment, achieving a 94% isolated yield. We envision that this process can be safely scaled up to industrial scales.

The robustness of TBD : PABA was further demonstrated by multiple deconstruction cycles. To interrogate this, we performed a catalyst cycling experiment where PET was continually glycolyzed under the action of our TBD : PABA catalyst. In a typical experiment, PET (200 mg, 1.04 mmol) was suspended in 10 equiv. EG (0.58 mL, 10.4 mmol) along with 5 mol% of TBD : PABA (14.4 mg, 0.052 mmol) in five 20 mL vial at 190 °C with stirring. The heterogeneous mixture became homogeneous after 1 hour and 1 vial was removed from heating and an aliquot was removed for ^{1}H NMR analysis followed by dilution with water (10 mL). A second portion of PET (200 mg) and 2 equiv. of EG was added to the remaining four 20 mL vials. All reactions were homogeneous after 1 h and this process was repeated five times. We observed near quantitative conversion of PET to soluble terephthalate species (95–99%) *via* ^{1}H NMR analysis of the aliquots (Fig. S31). Taken together, these results indicate that TBD : PABA suffers no discernible decrease in performance across five cycles of PET deconstruction at 190 °C, a trait that is highly desirable for industrial processes.

Another large advantage of TBD : PABA includes the cost and availability of PABA. PABA is a naturally occurring compound and is more commonly known as vitamin B10. As such, it is considered nontoxic with an LD$_{50}$ > 6 g kg^{-1} for rats,[25] and can readily be purchased from vendors and is even sold by commercial sources such as Amazon. PABA can also be purchased from commercial sources such as Millipore Sigma at a price of \$174 per kg, while other sources such as Ambeed lists prices as low as \$42 per kg. When we compared to our previously reported catalyst TBD : TFA, with its TFA cost at approximately \$326 per kg in the same vendor, Millipore Sigma, the cost for producing TBD : PABA is drastically lower, further improving its viability for commercialization. With its simplicity of catalyst preparation, cost effectiveness, relative nontoxicity (PABA only exhibits minor allergenic properties),[26] and availability as vitamin B10, TBD : PABA, compared to TBD : TFA, could be a more attractive candidate for scalable polymer deconstruction *via* glycolysis and other solvolysis in sustainable recycling processes.
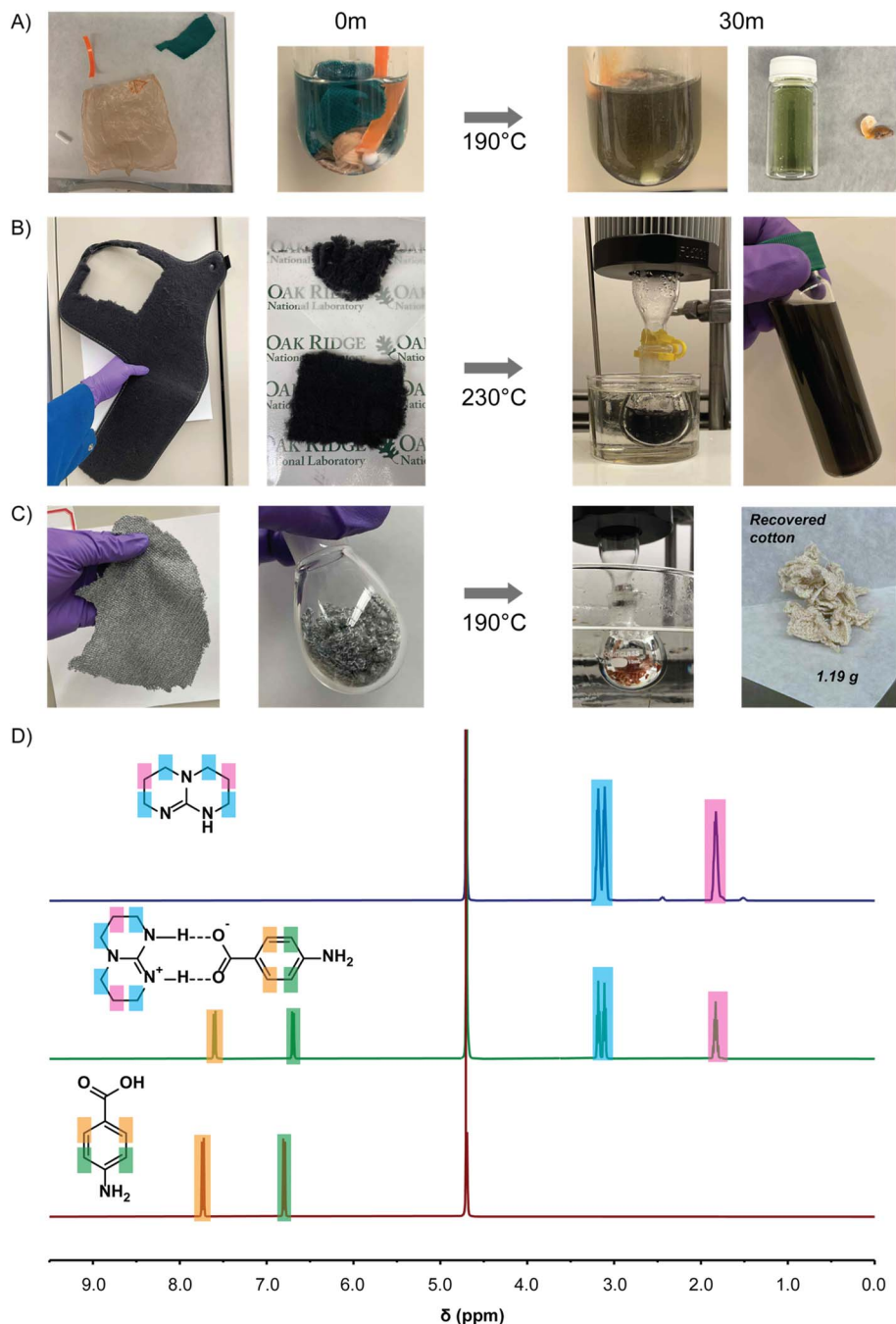
Fig. 4 (A) Deconstruction of mixed plastics and PET fabric achieved in 30 min and leaves unreactive plastics behind. (B) Deconstruction of fibers from automobile floor mat. (C) Deconstruction of 50 : 50 polyester : cotton blend clothing. (D) Stacked ^{1}H NMR spectra of TBD, PABA, & TBD : PABA.

Conclusions

We have demonstrated that tailoring catalyst structure and applying Hammett analysis revealed the role of electronic effects in catalytic efficiency, where electron-donating substituents moderately enhanced reaction kinetics. Additionally, thermal stability and melting temperatures for each acid–base pair correlated with their binding energies, as calculated by DFT, where higher binding energy corresponded with higher thermal stability and higher melting temperatures. The predictive nature of Hammett analysis guided the design of the TBD : PABA catalyst, enabling the selection of the most effective acid–base pair based on its electronic properties. TBD : PABA was the superior glycolysis catalyst due to its highest pK_a and lowest σ-value with lowest binding energy. TBD : PABA's lower cost and high thermal stability situate it as a desirable deconstruction catalyst for condensation polymers. The catalyst's thermal stability is advantageous for enabling deconstruction at higher

32118 | J. Mater. Chem. A, 2025, 13, 32111–32121

This journal is © The Royal Society of Chemistry 2025

temperatures without degradation, which is critical for processing the diverse polymers found in post-consumer waste. The use of TBD : PABA allowed effective sequential deconstruction of PC, PET, and Nylon 6,6 under temperature-dependent conditions. The ability to combine these deconstructions into a single reactor while taking a stepwise approach with different temperatures to enable sequential polymer deconstruction provides a possible route for mixed plastic deconstruction in scaled process. Compared to previously reported organocatalysts, TBD : PABA offers safer preparation and significant cost advantages, with PABA being far more economical and abundant as vitamin B-10. This affordability, combined with its robust performance and ease of synthesis, makes TBD : PABA a promising candidate for industrial chemical recycling, contributing to the development of scalable and sustainable solutions for managing polymer waste.

Materials

TFMBA, BA, MeOBA, TA and PABA and TBD were purchased from commercial sources and used without further purification unless specified. Poly(caprolactone), $M_n = 95\,000$ g mol^{-1}, and poly(bisphenol A carbonate), $M_w = 40\,000$ g mol^{-1}, used in the deconstruction kinetics study were purchased from Millipore Sigma. Poly(ethylene terephthalate) C60A, $M_w = 60\,000$ g mol^{-1}, was obtained from Eastman Chemical. Nylon 6,6 S240, $M_w = 84\,700$ g mol^{-1}, was purchased from Akulon.

Methods

Glycolysis of poly(caprolactone)

The glycolysis of poly(caprolactone) (PCL) was conducted as a homogeneous deconstruction using the following benzoic acid derivatives—4-aminobenzoic acid (PABA), 4-methoxybenzoic acid (MeOBA), p-toluic acid, benzoic acid (BA), and 4-(trifluoromethyl)-benzoic acid (TFMBA). Glycolysis reactions for the kinetics studies were done in a 5 : 1 : 0.05 ratio of ethylene glycol-to-repeat units of polycaprolactone-to-catalyst, respectively. Deconstruction reactions were performed by first dissolving 0.5 g of PCL in 7.5 mL of N-methyl-2-pyrrolidone (NMP) in a sealed 20 mL scintillation vial at 110 °C. Once the polymer was dissolved, 1.22 mL of ethylene glycol (EG) (21.9 mmol) was added to the vial. Upon the addition of EG, there is some visible precipitation of PCL, but further heating and stirring redissolves the polymer at the concentration the reactions were performed. Once the polymer solution was homogeneous again, 0.31 mg (0.219 mmol) of triazabicyclodecene (TBD) and an equimolar amount of the corresponding acid is added to the solution and sealed to allow the deconstruction to occur. To track reaction progress, aliquots of the reaction were taken at 1 h, 2 h, 3 h, 4 h, 5 h, 6 h, 8 h, and 16 h marks. These samples (~25 mg) were then subsequently dissolved in tetrahydrofuran (THF) for further analysis via size exclusion chromatography.

Sequential deconstruction of mixed plastics

Sequential deconstruction of three types of condensation polymers was achieved using heterogeneous deconstruction with

ethylene glycol and TBD : PABA as the catalyst. A stock solution of EG (50 mL, 0.89 mol), TBD : PABA (1.236 g, 4.47 mmol), and 1,3,5-trimethoxybenzene (0.5 g, 2.97 mmol) was prepared and stirred at room temperature until fully dissolved. PC (0.33 g) pellets, PET (0.33 g) powder, and Nylon 6,6 (0.33 g) pellets were added to a 15 mL pressure tube containing a stir bar. Then, 1.63 mL of the stock EG/catalyst solution was added into the pressure tube, before sealing and heating to the specific deconstruction temperature for each polymer. Unlike previous methods that targeted specific polymer repeat unit-to-EG/catalyst ratios, this sequential deconstruction methodology was designed to use a fixed amount of stock solution at each step, simulating a potential continuous reaction process.

PC was deconstructed first at 140 °C. The kinetics experiment was conducted using four separate pressure tubes, each allowing an aliquot to be removed every 30 minutes to monitor the formation of BPA. After removing an aliquot, the pressure tube was returned to the heating block and allowed to complete the 2 h reaction time. At the end of the PC deconstruction, PET and Nylon 6,6 remained intact, while BPA was present in the liquid fraction. The liquid fraction was vacuum filtered to isolate BPA, leaving unreacted PET and Nylon 6,6, which were then reintroduced into the pressure tube. Another 1.63 mL of stock solution was added, and the temperature was raised to 190 °C for PET deconstruction. Aliquots were similarly collected during this stage to monitor the formation of BHET. During the PET reaction, Nylon 6,6 may melt and disperse into the liquid fraction, losing its pellet form. However, since BHET is soluble in chloroform, it can be extracted from the Nylon 6,6 by washing and filtering with chloroform. Finally, Nylon 6,6 was deconstructed at 230 °C into its respective monomers.

Automobile floor mat fibers deconstruction

An automobile floor mat was pre-treated via the removal of its fibers comprised of Nylon and polyester ($M_n = 32\,300$ g mol^{-1}) from backing. Glycolysis reactions for the fibers were done in a 20 : 1 : 0.05 ratio of EG-to-repeat units of PET-to-catalyst, respectively. The separated fibers (1 g, 5.2 mmol) were loaded into a 10 mL round-bottom flask (RBF) along with a stir bar, 20 equivalents of EG (5.8 mL, 104 mmol), and 5 mol% of TBD : PABA (71.9 mg, 0.26 mmol). The RBF was equipped with a Findenser, and the reaction vessel heated at 230 °C and allowed to reflux for 2 hours. Once the reaction had completed, the system was allowed to cool, and the crude reaction mixture was diluted with HFIP (50 mL) and aliquots were removed for HFIP-SEC analysis. SEC traces depicting the fibers before and after glycolysis are shown in Fig. S29. Photographs showing various steps in the deconstruction process shown in Fig. 4B.

50% cotton 50% polyester fabric deconstruction

A 50 : 50 cotton : polyester fabric was deconstructed in a 20 : 1 : 0.05 ratio of EG-to-repeat units of PET-to-catalyst, respectively. In a typical reaction, a 25 mL RBF was charged with 2.5 g of the fabric (1.25 g polyester, 6.5 mmol), a stir bar, 20 equivalents of EG (7.27 mL, 130 mmol), and 5 mol% TBD : PABA (90 mg, 0.325 mmol). The RBF was equipped with a Findenser and the

This journal is © The Royal Society of Chemistry 2025

J. Mater. Chem. A, 2025, 13, 32111–32121 | 32119

reaction vessel heated at 190 °C with stirring. The reaction is allowed to reflux for two hours, after which the system is cooled to room temperature. The crude reaction mixture was diluted with THF, to recover deconstructed polyester, and subsequently vacuum filtered to isolate unreacted cotton. The recovered cotton fibers were then washed with more THF and dried for 16 h under high vacuum. The THF solution of deconstructed polyester in THF was concentrated to dryness, and a 5 mg sample was dissolved in HFIP for SEC analysis *via* HFIP GPC. Photographs showing various steps in the deconstruction process shown in Fig. 4C. SEC traces of the shirt before and the recovered residue shown in Fig. S30.

Nylon 6,6 TBD : PABA deconstruction and thermal degradation

Nylon 6,6 ($M_n = 70\,700$ g mol^{-1}) was deconstructed in a 10 : 1 : 0.05 ratio of EG-to-repeat units of Nylon 6,6-to-catalyst and 10 : 1 : 0 ratio (no catalyst). In a typical reaction, a 10 mL RBF was charged with Nylon 6,6 pellets (1 g, 4.4 mmol) a stir bar, 10 equivalents of EG (2.47 mL, 44 mmol), and 5 mol% TBD : PABA (61 mg, 0.22 mmol) or no TBD : PABA. The RBF is equipped with a Findenser, and the vessel is immersed in an oil bath at 230 °C and allowed to reflux. The deconstruction kinetics are monitored by removing aliquots from the reaction solution every 30 minutes. The aliquots are then diluted with HFIP and analyzed by SEC *via* HFIP GPC. Plot depicting M_n *vs.* reaction time shown in Fig. S28.

Size exclusion chromatography

Size exclusion chromatography (SEC) for PCL deconstructions were performed on a Tosoh EcoSEC Elite system. The instrument is equipped with two Tosoh TSKgel Super AWM-H columns (15 cm × 6 mm ID, 9 μm pore size), an integrated differential RI detector, and has a mobile phase of THF (HPLC grade) with a flow rate of 0.6 mL min^{-1}. Weight average molecular weight (M_w), number average molecular weight (M_n), and dispersity ($Đ = M_w/M_n$) are all calculated based on PMMA standards. SEC analysis was performed on an Agilent 1260 Infinity II LC system equipped with an Agilent MiniMIX-C Guard column (PL Gel 5 μM, 50 × 4.6 mm) and two Agilent PL HFIPgel (250 × 4.6 mm, 9 μm). HFIP was used as the mobile phase at a flow rate of 0.3 mL min^{-1}. Molecular weights were determined from RI detection (Table S1).

Organosalt synthesis

The salts for TBD with TFMBA, BA, MeOBA, and TA were prepared by dissolving TBD and the respective acids in chloroform in equimolar ratios. Once the solution appears to be homogeneous, chloroform is evaporated, and the resulting salt is dried in a vacuum oven overnight to remove excess solvents. The preparation of TBD : aminobenzoic acid salt was done by dissolving TBD and aminobenzoic acid in THF in separated beakers. Once both solutions have been prepared, a stir bar is added to the beaker with TBD. The aminobenzoic acid solution was poured into the TBD beaker while stirring and resulted in precipitating

out the salt. The resulting salt is vacuum filtered and washed with additional THF before vacuum drying overnight.

Catalyst cycling

Catalyst cyclability was monitored by five different reactions. Glycolysis reactions were performed in a 10 : 1 : 0.05 ratio of EG-to-repeat units of PET-to-catalyst, respectively. In a typical experiment, a six-vial heating block is set to 190 °C. Five 20 mL vials were charged with PET (200 mg, 1.04 mmol), 10 equivalents of EG (0.58 mL, 10.4 mmol), and 5 mol% TBD : PABA (14.4 mg, 0.052 mmol) and loaded into the heating block and capped with a rubber septa. Each vial is stirred at 190 °C. After an hour, a single vial is removed from heating and an aliquot of the homogeneous solution is taken for ^{1}H NMR analysis followed by dilution of the bulk reaction with water (10 mL). The remaining vials are then charged with an additional portion of PET (200 mg, 1.04 mmol) and 2 equivalents of EG (0.116 mL, 2.08 mmol) and allowed to react once more for an hour. This process is repeated until the last vial has gone through five successive deconstruction reactions. The aliquots were dissolved in DMSO-d$_6$ followed by addition of external standard mesitylene (5 μL, 0.035 mmol) and subject to ^{1}H NMR spectroscopic analysis. Bar chart depicting conversion to soluble terephthalate (*i.e.*, BHET, dimeric, & trimeric) species shown in Fig. S31.

Nuclear magnetic resonance spectroscopy

^{1}H NMR was obtained using Bruker Avance III 400 NMR spectrometer operating at 400 MHz. Trimethoxybenzene was used as an internal standard for the deconstruction of the various step-growth polymers, and unless it was specified, CDCl$_3$ was used as the solvent. To determine NMR conversion for catalyst cycling, the theoretical maximum weight of BHET at the end of each cycle was determined assuming full conversion. The relative wt% of BHET, with respect to total reaction weight, was calculated (Table S2). With these theoretical maximum wt% values determined, we determined the maximum possible BHET in each aliquot (Table S2). The amount of BHET and other soluble aromatics for each cycle were determined using added external standard and compared to the theoretical total to determine conversion. Bar chart depicting these calculated conversions are shown in Fig. S31.

Thermogravimetric analysis

Thermogravimetric analysis (TGA) was performed using a TGA55 manufactured by TA Instruments. The instrument measures all TGA samples under a constant flow of nitrogen, and all samples were run at a heating rate of 5.0 °C min^{-1} from room temperature to 600 °C.

Differential scanning calorimetry

Differential scanning calorimetry (DSC) was performed using a TA Instruments Discovery Series TGA55. Samples of ~5 mg are loaded onto T-zero pans and heated at rates of 10 °C min^{-1}. T_g and T_m are calculated based on points of inflection.

32120 | *J. Mater. Chem. A*, 2025, 13, 32111–32121

This journal is © The Royal Society of Chemistry 2025

Density functional theory (DFT)

All-electron density functional theory (DFT) calculations were carried out using the NWChem suite of codes (version 7.0.2).[27] For the DFT calculations, the hybrid meta functional m06-2x[28] and the aug-cc-pvdz basis set[29] were used (we also checked binding energy trends using a aug-cc-pvtz basis set). Full geometry optimization for TBD paired with BA and benzoic acid derivatives (BA, PABA, MeOBA, TA, TFMBA) was performed with tight convergence criteria. The binding energy was computed as the difference between the optimized TBD–benzoic acid pairs and the optimized TBD and benzoic acids molecules. Since we were looking for trends, we did not correct the binding energies for basis set superposition error. These calculations were done in the gas-phase agnostic of solvent.

Conflicts of interest

The authors declare no conflicts of interest.

Data availability

The data supporting this article have been included as part of the SI. See DOI: https://doi.org/10.1039/d5ta05717e.

Acknowledgements

References

1 Global plastic production, Statista, https://www.statista.com/statistics/282732/global-production-of-plastics-since-1950/, accessed 27 January 2025.

2 Plastic pollution is growing relentlessly as waste management and recycling fall short, says OECD, OECD, https://www.oecd.org/en/about/news/press-releases/2022/02/plastic-pollution-is-growing-relentlessly-as-waste-management-and-recycling-fall-short.html.

3 K. Nixon, Z. Schyns, Y. Luo, M. Ierapetritou, D. Vlachos, L. T. J. Korley and T. Epps III, Nat. Chem. Eng., 2024, 1, 615–626.

4 J. Zheng, M. Arifuzzaman, X. Tang, X. Chen and T. Saito, Mater. Horiz., 2023, 10, 1608–1624.

5 Z. Schyns and M. Shaver, Macromol. Rapid Commun., 2021, 42, 2000415.

6 K. Fukushima, O. Coulembier, J. Lecuyer, H. Almegren, A. Alabdulrahman, F. Alsewailem, A. McNeil, P. Dubois,

R. Waymouth, H. Horn, J. Rice and J. Hedrick, J. Polym. Sci., Part A: Polym. Chem., 2011, 49, 1273–1281.

7 M. Arifuzzaman, B. Sumpter, Z. Demchuk, C. Do, M. Arnould, M. Rahman, P. Cao, I. Popovs, R. Davis, S. Dai and T. Saito, Mater. Horiz., 2023, 10, 3360–3368.

8 C. Jehanno, I. Flores, A. Dove, A. Müller, F. Ruipérez and H. Sardon, Green Chem., 2018, 20, 1205–1212.

9 G. Coates and Y. Getzler, Nat. Rev. Mater., 2020, 5, 501–516.

10 M. Hong and E. Chen, Green Chem., 2017, 19, 3692–3706.

11 J. Kim, G. Lee and A. Lee, J. Polym. Sci., 2024, 62, 42–91.

12 A. Hyde, R. Calabria, R. Arvary, X. Wang and A. Klapars, Org. Process Res. Dev., 2019, 23, 1860–1871.

13 F. Kilens, A. Olazabal, D. Mantione, A. Basterretxea, H. Sardon and C. Jehanno, ChemCatChem, 2024, 16, e202400215.

14 L. Hammett, J. Am. Chem. Soc., 1937, 59, 96–103.

15 K. Fukushima, D. Coady, G. Jones, H. Almegren, A. Alabdulrahman, F. Alsewailem, H. Horn, J. Rice and J. Hedrick, J. Polym. Sci., Part A: Polym. Chem., 2013, 51, 1606–1611.

16 C. Zhu, L. Yang, C. Chen, G. Zeng and W. Jiang, Phys. Chem. Chem. Phys., 2023, 25, 27936–27941.

17 C. Rogers, T. Dickerson, A. Brogan and A. K. Janda, J. Org. Chem., 2005, 70, 3705–3708.

18 B. Dong, G. Xu, R. Yang and Q. Wang, Chem.–Asian J., 2022, 17, e202200667.

19 J. Demarteau, A. Epstein, P. Christensen, M. Abubekerov, H. Wang, S. Teat, T. Seguin, C. Chan, C. Scown, T. Russell, J. Keasling, K. Persson and B. Helms, Sci. Adv., 2022, 8, eabp8823.

20 Z. Zhang, J. Wang, X. Ge, S. Wang, A. Li, R. Li, J. Shen, X. Liang, T. Gan, X. Han, X. Zheng, X. Duan, D. Wang, J. Jiang and Y. Li, J. Am. Chem. Soc., 2023, 145, 22836–22844.

21 H. Luo, G. Baker, J. Lee, R. Pagni and S. Dai, J. Phys. Chem. B, 2009, 113, 4181–4183.

22 M. Yoshizawa, W. Xu and C. Angell, J. Am. Chem. Soc., 2003, 125, 15411–15419.

23 T. Kwon, H. Jeong, M. Kim, S. Jung and I. Ro, Langmuir, 2024, 40, 17212–17238.

24 K. Kim, D. Dhevi, J. Lee, Y. Cho and E. Choe, Polym. Degrad. Stab., 2006, 91, 1545–1555.

25 Safety data sheet (4-aminobenzoic acid), Sigma-Aldrich, https://www.sigmaaldrich.com/US/en/sds/aldrich/100536, accessed 27 January 2025.

26 C. Mathias, H. Mailbach and J. Epstein, Arch. Dermatol., 1978, 114, 1665–1666.

27 M. Valiev, E. Bylaska, N. Govind, K. Kowalski, T. Straatsma, H. Van Dam, D. Wang, J. Nieplocha, E. Apra, T. Windus and W. de Jong, Comput. Phys. Commun., 2010, 181, 1477–1489.

28 Y. Zhao and D. G. Truhlar, J. Chem. Phys., 2006, 125, 194101.

29 T. H. Dunning Jr., J. Chem. Phys., 1989, 90, 1007.

This journal is © The Royal Society of Chemistry 2025

J. Mater. Chem. A, 2025, 13, 32111–32121 | 32121